

Electronic Supplementary Information (ESI)

**Multifunctional Cu-Ag<sub>2</sub>S nanoparticles with high photothermal conversion efficiency for photoacoustic imaging guided photothermal therapy *in vivo***

Lile Dong,<sup>a,b</sup> Guanming Ji,<sup>c</sup> Yu Liu,<sup>a,d</sup> Xia Xu,<sup>a,d</sup> Pengpeng Lei,<sup>a,d</sup> Kaimin Du,<sup>a,b</sup>

Shuyan Song,<sup>a</sup> Jing Feng<sup>\*a</sup> and Hongjie Zhang<sup>\*a</sup>

<sup>a</sup> State Key Laboratory of Rare Earth Resource Utilization, Changchun Institute of Applied Chemistry, Chinese Academy of Science, Changchun 130022, PR China.

<sup>b</sup> University of Science and Technology of China, Hefei 230026, PR China.

<sup>c</sup> Department of Radiology, China-Japan Union Hospital of Jilin University, Changchun 130041, China

<sup>d</sup> *University of Chinese Academy of Sciences, Beijing 100049, China.*

**Corresponding Authors**

Tel.: +86 431 85262127; fax: +86 431 85698041.

\*E-mail: [fengj@ciac.ac.cn](mailto:fengj@ciac.ac.cn); [hongjie@ciac.ac.cn](mailto:hongjie@ciac.ac.cn)

## 1. Experimental

### 1.1 Materials and characterization

Copper (II) acetylacetonate (98%), oleylamine (C18 content 80–90%), and polyvinylpyrrolidone (PVP 58000) were purchased from Aladdin Industrial Corporation (Shanghai, China). Silver nitrate ( $\text{AgNO}_3$ , 99.8%), sulfur powder (S, 99.5%), chloroform (99.0%), ethanol (99.7%), dichloromethane (99.0%), ether (99.0%), and cyclohexane (99.0%) were purchased from Beijing Chemical Regents. All the reagents were analytical grade and used directly without further purification. Deionized water was used throughout the experiments.

Low-/high-resolution transmission electron microscopy (TEM) images were obtained with a FEI TECNAI G2 high-resolution transmission electron microscope operating with a field-emission gun operating at 200 kV. Powder X-ray diffraction (XRD) patterns were obtained on a D8 ADVANCE X-ray diffractometer with Cu K $\alpha$  radiation ( $\lambda = 1.5418 \text{ \AA}$ ) with an operation voltage and current maintained at 40 kV and 40 mA. Energy-dispersive X-ray (EDX) spectrometry was obtained on field-emission scanning electron microscope (FE - SEM, S-4800, Hitachi). X-ray photoelectron spectroscopy (XPS) was obtained on a VG ESCALAB MKII spectrometer. Inductively couple plasma mass spectrometry (ICP-MS) was carried out on an ELAN 9000/DRC. Inductively couple plasma-optical emission spectrometer (ICP-OES) was taken on a PerkinElmer ICP instrument. Fourier transform infrared spectroscopy (FT-IR) was recorded on a PerkinElmer 580B IR spectrophotometer using the KBr pellet technique. The absorption spectrum was recorded on a Shimadzu UV-3600 UV-VIS-NIR spectrophotometer.

### 1.2 Synthesis of $\text{Cu}_{2-x}\text{S}$ -1 NPs

The as-prepared  $\text{Cu}_{2-x}\text{S}$ -1 NPs were synthesized by a modified literature procedure. Briefly, 2 mmol of sulfur was dissolved in 12 mL of oleylamine, and stirred at 70 °C for 0.5 h in an oil bath. Subsequently, this solution was added dropwise into 20 mL chloroform solution containing 5 mL oleylamine and 2 mmol  $\text{Cu}(\text{acac})_2$ . After the mixture was further stirred for another 0.5 h. and the  $\text{Cu}_{2-x}\text{S}$ -1 NPs were isolated by

centrifugation, washed two times with ethanol and chloroform, and re-dispersed in cyclohexane (40 mL) for later use.

### **1.3 Synthesis of Ag<sub>2</sub>S product**

4 mL chloroform solution containing 1 mL oleylamine and 0.5 mmol AgNO<sub>3</sub> was added dropwise into 3 mL oleylamine and 10 mL cyclohexane solution of the Cu<sub>2-x</sub>S-1 NPs and stirred at 70 °C for 0.5 h. The Ag<sub>2</sub>S NPs were obtained by centrifugation, washed with ethanol and cyclohexane, and re-dispersed in cyclohexane (10 mL) for later use.

### **1.4 Synthesis of Cu-Ag<sub>2</sub>S NPs**

1 mmol of sulfur was dissolved in 3 mL of oleylamine, and rapidly injected into a 10 mL cyclohexane solution of the as-synthesized Cu<sub>2-x</sub>S-1 NPs at 70 °C and stirred at this temperature for 10 min in an oil bath. Then 4 mL chloroform solution containing 1 mL oleylamine and 0.5 mmol AgNO<sub>3</sub> was added dropwise into the above solution and stirred at 70 °C for 0.5 h. The Cu-Ag<sub>2</sub>S NPs were obtained by centrifugation, washed with ethanol and cyclohexane, and re-dispersed in cyclohexane (10 mL) for later use.

### **1.5 Surface modification of Cu-Ag<sub>2</sub>S NPs**

150 mg of Cu-Ag<sub>2</sub>S NPs were first dispersed in 100 mL of dichloromethane. Then, 1 g of PVP was added and the mixture was stirred at room temperature for 10 min. Cu-Ag<sub>2</sub>S/PVP NPs were precipitated by adding ether and obtained by centrifugation, and the re-dispersed in PBS solution. The resulting solution was centrifugation at a high speed and then the obtained solution was transferred into dialysis bags and dialyzed against PBS solution for 72 h. Finally, the Cu-Ag<sub>2</sub>S/PVP NPs were dispersed in PBS solution and kept at 4 °C for later use.

### **1.6 Photothermal experiments in PBS solution**

1.0 mL of PBS solution containing Cu-Ag<sub>2</sub>S/PVP NPs with various Cu concentrations (0, 6.25, 12.5, 25, 50, and 100 ppm) were placed in a quartz cuvette and then irradiated by an 808 nm laser (1.58 W cm<sup>-2</sup>, 10 min). The solution temperature was measured every 2 s by a thermocouple microprobe.

### **1.7 *In vitro* cytotoxicity assessment**

*In vitro* cytotoxicity of Cu-Ag<sub>2</sub>S/PVP NPs was evaluated by MTT assay of 4T1 murine breast tumor cells. Cells were seeded into 96-well cell culture plates (10<sup>4</sup> per well) at 37 °C and 5% CO<sub>2</sub> for 24 h. After 24 h of incubation, the DMEM was taken out from the wells, and the cells were washed for three times with PBS solution. The PBS solution of Cu-Ag<sub>2</sub>S/PVP NPs with various Cu concentrations (0, 0.78, 1.56, 3.12, 6.25, 12.5, 25, 50, 100 and 200 ppm) were added into the medium. Then, the cells were incubated at 37 °C and 5% CO<sub>2</sub> for 24 h. Thereafter, MTT (10 µL, 5 mg mL<sup>-1</sup>) solutions was added into each well and the plate was incubated for 4 h at 37 °C and 5% CO<sub>2</sub> in order to form a purple formazan dye, which was dissolved in DMSO for 15 min after removing the medium. Finally, the enzyme-linked immunosorbent assay reader was used to measure the optical absorbance of the colored solution at 570 nm. Each experiment was repeated three.

### **1.8 *In vitro* cellular uptake assay**

4T1 murine breast tumor cells were seeded in 1 mL of medium in each well (3.5 cm in diameter) of a 6-well plate at the density of 10<sup>5</sup> cells per well cells. After 24 h of incubation at 37 °C, the medium was replaced with fresh medium containing Cu-Ag<sub>2</sub>S/PVP NPs with Cu concentration of 25, 50 and 100 ppm. After another 24 h of incubation at 37 °C, the medium was removed; the cells were washed three times with PBS (pH = 7.4) and trypsinized. Then, the cell suspensions were digested using 1 mL of concentrated HNO<sub>3</sub>10% (v/v) and the intracellular Cu concentration used for ICP-MS measurement.

### **1.9 *In vitro* photothermal ablation of cancer cells**

4T1 murine breast tumor cells were seeded into 96-well cell culture plates (10<sup>4</sup> per well) at 37 °C and 5% CO<sub>2</sub> for 24 h. Then the cells were treated with PBS solution containing Cu-Ag<sub>2</sub>S/PVP NPs with various Cu concentrations (0, 0.78, 1.56, 3.12, 6.25, 12.5, 25, 50, 100 and 200 ppm). Then, the cells were irradiated by an 808-nm laser with a power density of 1.58 W cm<sup>-2</sup> for 10 min. The cell viabilities were measured by MTT assays.

### **1.10 Live/dead staining kit**

4T1 murine breast tumor cells ( $4 \times 10^4$  cells per well) were placed in a 24-well plate. After overnight incubation, culture medium was removed and cells were washed three times with PBS. Then cells were treated with PBS solution containing only or Cu-Ag<sub>2</sub>S/PVP NPs with various Cu concentrations (0, 3.12, 6.25, 12.5, 25, 50, 100 and 200 ppm) incubated for 6 h. Then they were irradiated under 808 nm laser irradiation ( $1.58 \text{ W cm}^{-2}$ ) for 10 min. After 18 h incubation, 4T1 murine breast tumor cells were washed with PBS and stained with calcein AM (2  $\mu\text{M}$ ) and propidium iodide (PI, 4  $\mu\text{M}$ ) for 2 hours and observed using NikonTi-S fluorescence microscope (Tokyo, Japan), live cells showed green color and dead ones exhibited red color.

### **1.11 Animal Experiments**

Female Kunming mice were obtained from the Laboratory Animal Center of Jilin University (China). All *in vivo* experiments were conducted in strict adherence the criteria of the Regional Ethics Committee for Animal Experiments. The tumor models were established by subcutaneous injection of H22 cells in the left axilla of each Kunming mouse.

### **1.12 *In vitro* and *in vivo* PA imaging**

1.0 mL of PBS solution containing Cu-Ag<sub>2</sub>S/PVP NPs with various Cu concentrations (12.5, 25, 50, and 100 ppm) embedded in agar gel cylinders with a diameter of 1 cm were performed quantitatively to investigate the PA signal. The excitation wavelength of 808 nm was adopted. The tumor-bearing mice were used for the *in vivo* PA imaging. 100  $\mu\text{L}$  of PBS solution containing Cu-Ag<sub>2</sub>S/PVP NPs with Cu concentration of 200 ppm were injected intravenously into the tumor-bearing mice, the PA images were performed at different time intervals (pre, 2 h, 6 h and 24 h).

### **1.13 *In vivo* photothermal effect**

100  $\mu\text{L}$  of PBS solution containing Cu-Ag<sub>2</sub>S/PVP NPs with Cu concentration of 200 ppm were intratumoral injected into the tumor-bearing mice. Then, the tumor was exposed to an 808 nm laser ( $1.58 \text{ W cm}^{-2}$ ) for 10 min and imaged by an IR thermal imaging camera at different time intervals (pre, 1, 3, 5, and 10 min). The tumor-bearing mice were also intravenous injected with PBS solution containing Cu-Ag<sub>2</sub>S/PVP NPs at the same dose (100  $\mu\text{L}$ , 200 ppm). Then, the tumor was also

exposed to an 808 nm laser ( $1.58 \text{ W cm}^{-2}$ ) for 10 min and imaged by an IR thermal imaging camera at different time intervals (pre, 0.5 h, 2 h, 6 h, and 24 h).

#### **1.14 *In vivo* biodistribution of Cu-Ag<sub>2</sub>S/PVP NPs**

100  $\mu\text{L}$  of PBS solution containing Cu-Ag<sub>2</sub>S/PVP NPs with Cu concentration of 200 ppm were intravenous injected into the tumor-bearing mice. At 0 h, 2 h, 6 h, 1d, 3d and 7d after administration, the tumor-bearing mice were euthanized for analysis of the systemic distribution of Cu-Ag<sub>2</sub>S/PVP NPs ( $n = 3$  at each time point). After digesting the major organs (heart, liver, spleen, lung, kidney, and tumor) and feces with aqua regia solution for 6 h. The Ag and Cu amount per unit mass was quantified by ICP-MS.

#### **1.15 *In vivo* photothermal therapy and histology examinations**

The tumor-bearing mice (the tumors volume were about  $200 \text{ mm}^3$ ) were randomly allocated into four treatment groups (three animals per treatment group): 100  $\mu\text{L}$  of PBS solution containing Cu-Ag<sub>2</sub>S/PVP NPs with Cu concentration of 200 ppm were intravenous injected into the tumor-bearing mice and treated with 808 nm irradiation ( $1.58 \text{ W cm}^{-2}$ , 10 min) after 24 h as group I (Cu-Ag<sub>2</sub>S/PVP + NIR); 100  $\mu\text{L}$  of PBS solution were intravenous injected into the tumor-bearing mice and treated with 808 nm irradiation ( $1.58 \text{ W cm}^{-2}$ , 10 min) after 24 h as group II (NIR); 100  $\mu\text{L}$  of PBS solution containing Cu-Ag<sub>2</sub>S/PVP NPs with Cu concentration of 200 ppm were intravenous injected into the tumor-bearing mice as group III (Cu-Ag<sub>2</sub>S/PVP); 100  $\mu\text{L}$  of PBS solution were intravenous injected into the tumor-bearing mice as group IV (PBS). The tumor sizes were measured by a caliper every day after photothermal treatment and calculated according to the formulation  $V = Dd^2/2$  ( $D$  and  $d$  represent length and width of the tumor, respectively). Relative tumor volumes were calculated as  $V/V_0$ , where  $V_0$  was the tumor volume when the treatment was initiated. We also collected the body weight data of the mice on a daily basis for 14 d. The tumor-bearing mice were killed 14 day after the laser treatment. Then, the organs (heart, liver, spleen, lung, and kidney) obtained from group I, group IV and healthy mice and the tumors obtained from group I and group IV were stained with H&E for histological analysis.

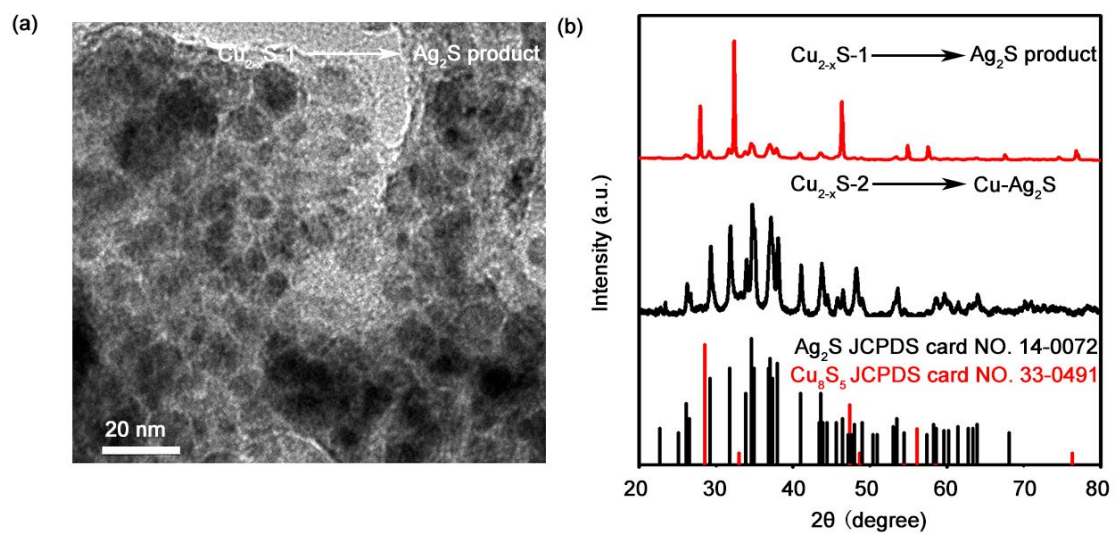


**Fig. S1** (a) TEM images of as-synthesized  $\text{Ag}_2\text{S}$  product using  $\text{Cu}_{2-x}\text{S}$ -1 as template; (b) the corresponding XRD patterns of as-synthesized  $\text{Ag}_2\text{S}$  product and  $\text{Cu-Ag}_2\text{S}$  NPs.

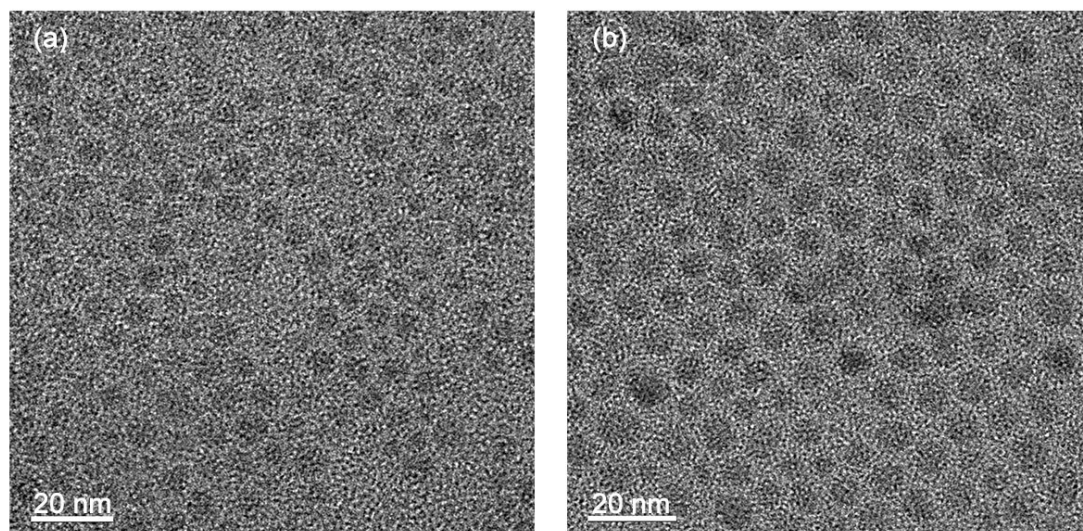


**Fig. S2** TEM images of  $\text{Cu}_{2-x}\text{S}$ -1 NPs (a) and  $\text{Cu}_{2-x}\text{S}$ -2 NPs (b).



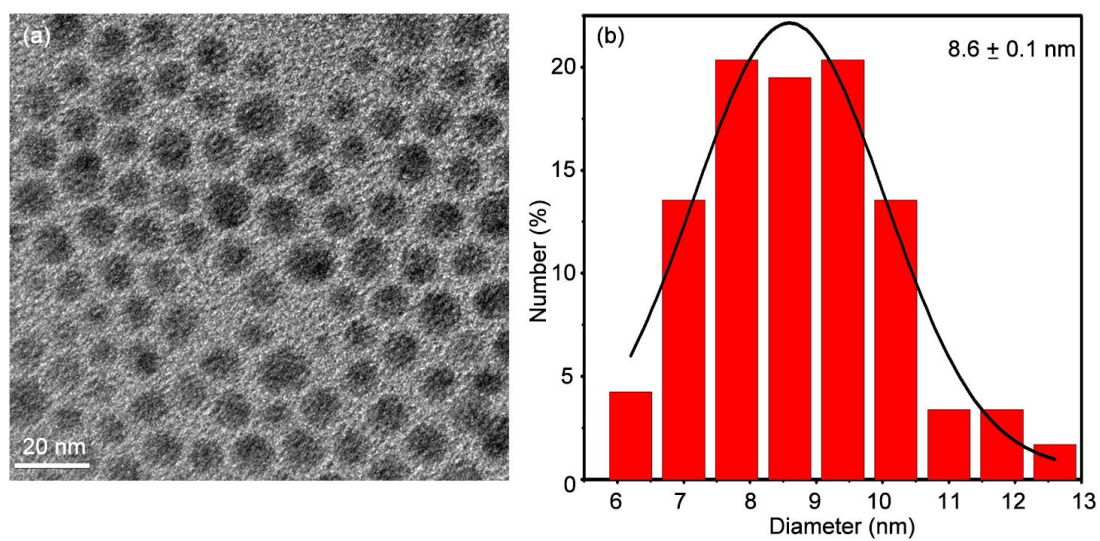


**Fig. S3** TEM images of Cu-Ag<sub>2</sub>S NPs (a) and the corresponding size distribution histograms (b).

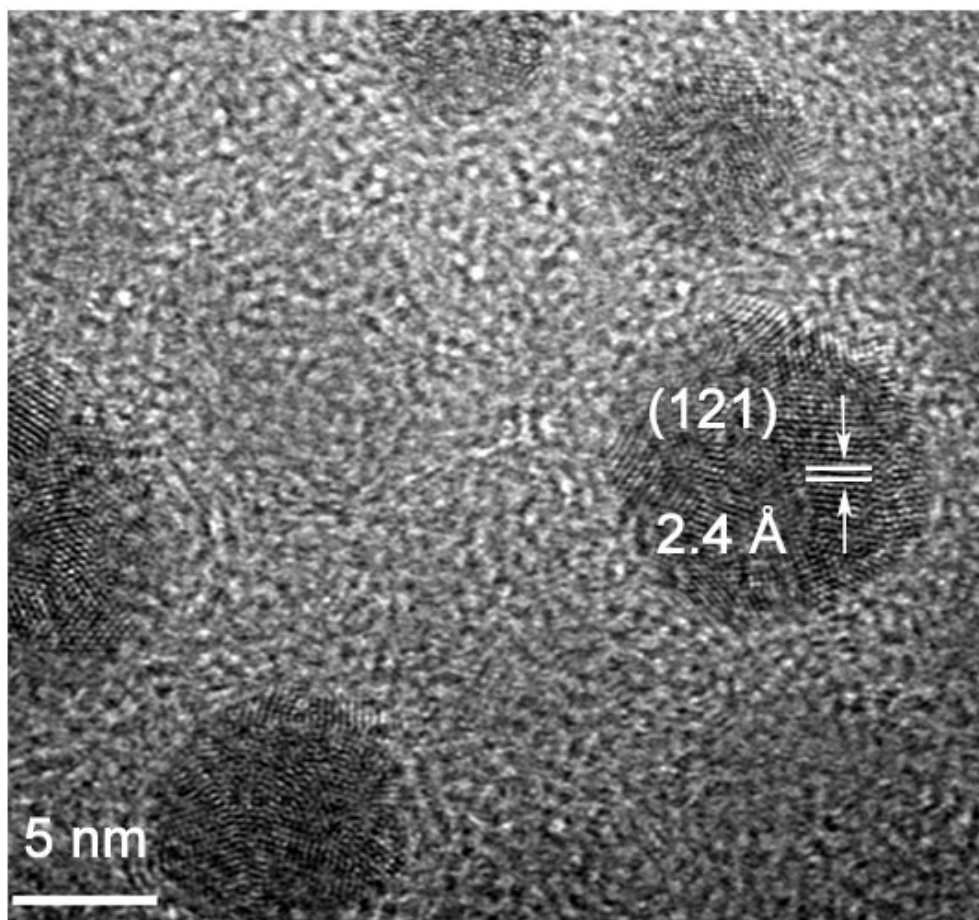


**Fig. S4** High-resolution transmission electron microscopy (HRTEM) image of Cu-Ag<sub>2</sub>S NPs.

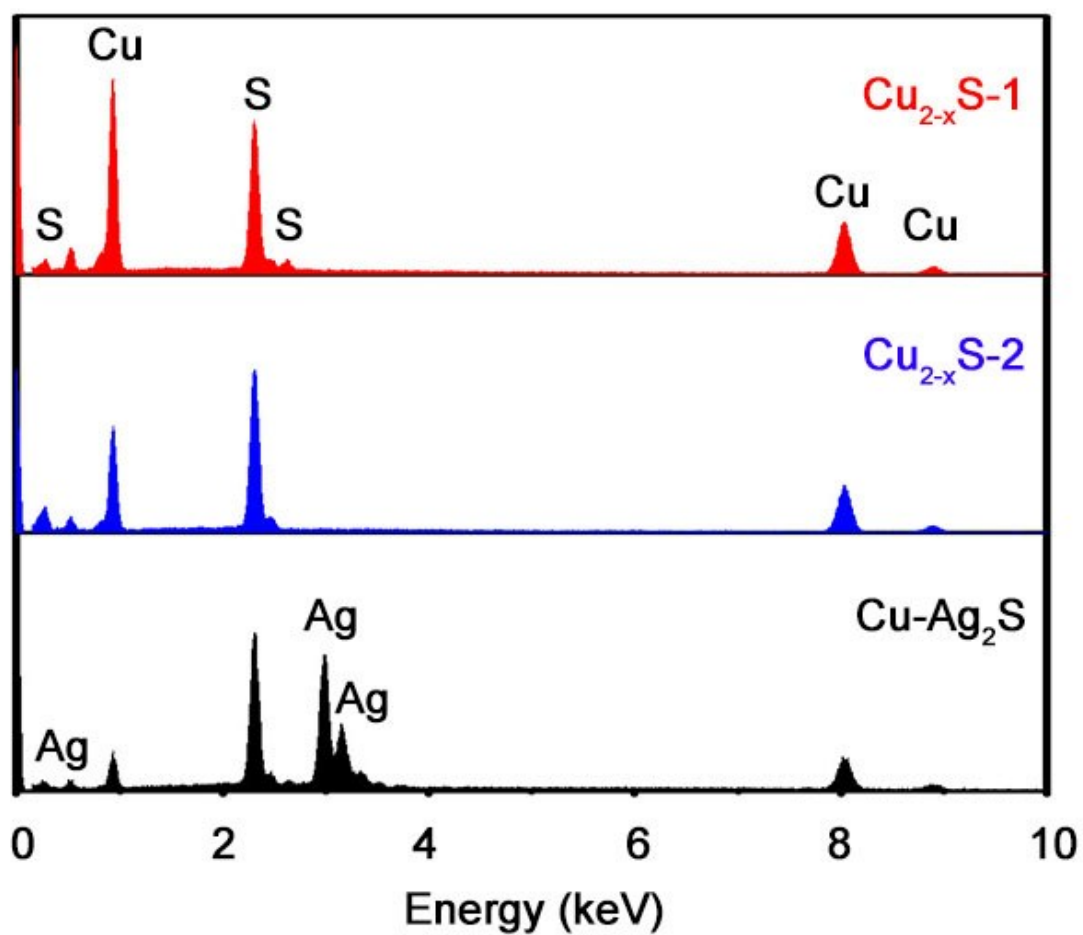


**Fig. S5** EDX spectra of  $\text{Cu}_{2-x}\text{S-1}$  NPs,  $\text{Cu}_{2-x}\text{S-2}$  NPs, and  $\text{Cu-Ag}_2\text{S}$  NPs.

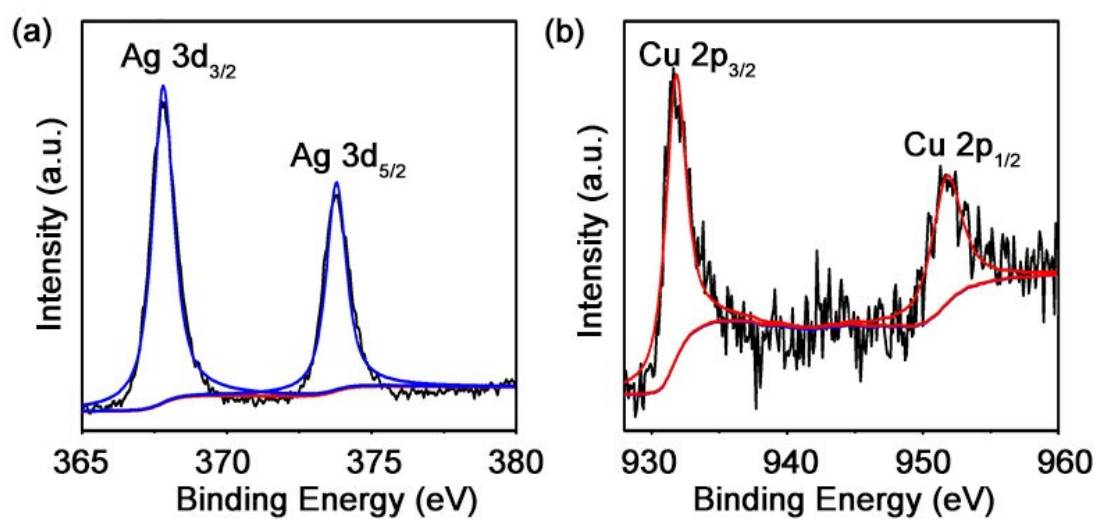


**Fig. S6** XPS spectra of Ag 3d (a) and Cu 2p (b) in Cu-Ag<sub>2</sub>S NPs.

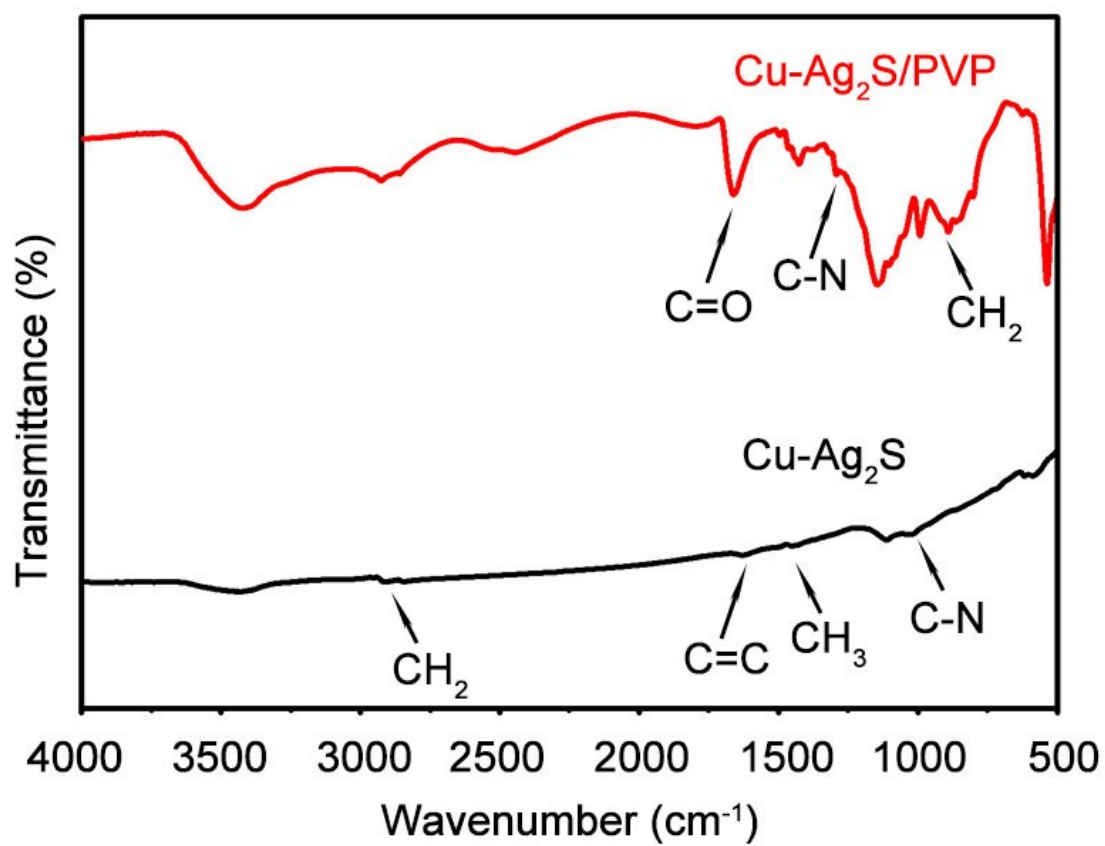


**Fig. S7** FTIR spectra of  $\text{Cu-Ag}_2\text{S}$  and  $\text{Cu-Ag}_2\text{S/PVP}$  NPs.

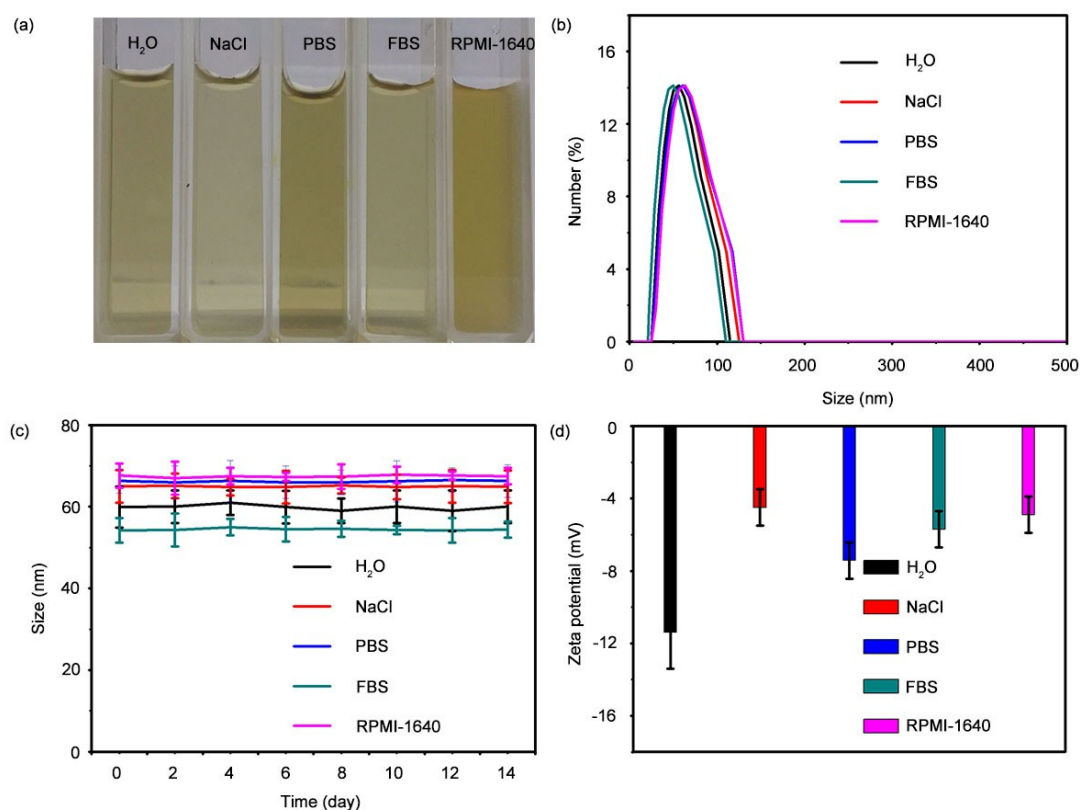


**Fig. S8** (a) The photographs of Cu-Ag<sub>2</sub>S/PVP NPs dispersed in water, 0.9% NaCl solution, PBS solution, FBS solution and RPMI-1640; (b) Hydrodynamic sizes of Cu-Ag<sub>2</sub>S/PVP NPs dispersed in water, 0.9% NaCl solution, PBS solution, FBS solution and RPMI-1640; (c) Hydrodynamic size changes of Cu-Ag<sub>2</sub>S/PVP NPs dispersed in water, 0.9% NaCl solution, PBS solution, FBS solution and RPMI-1640 for 15 d; (d) Zeta potentials of Cu-Ag<sub>2</sub>S/PVP NPs dispersed in water, in water, 0.9% NaCl solution, PBS solution, FBS solution and RPMI-1640.

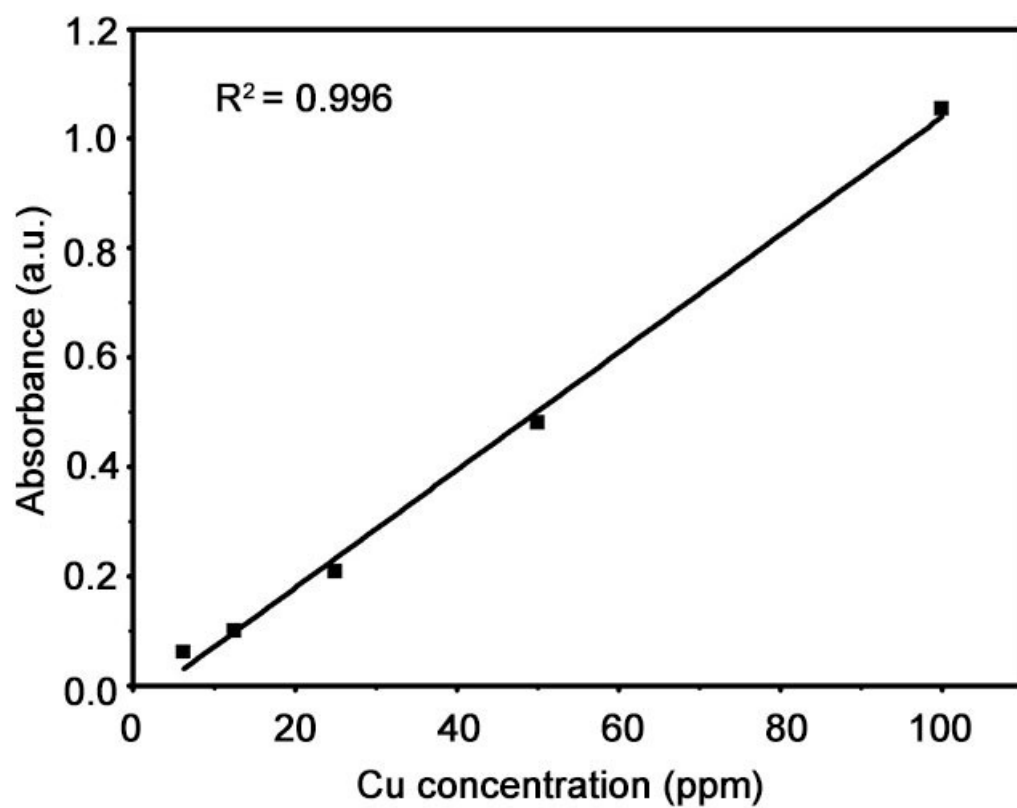


**Fig. S9** Linear fitting plot of NIR absorbance at 808 nm versus Cu concentrations of Cu-Ag<sub>2</sub>S/PVP NPs PBS solution.

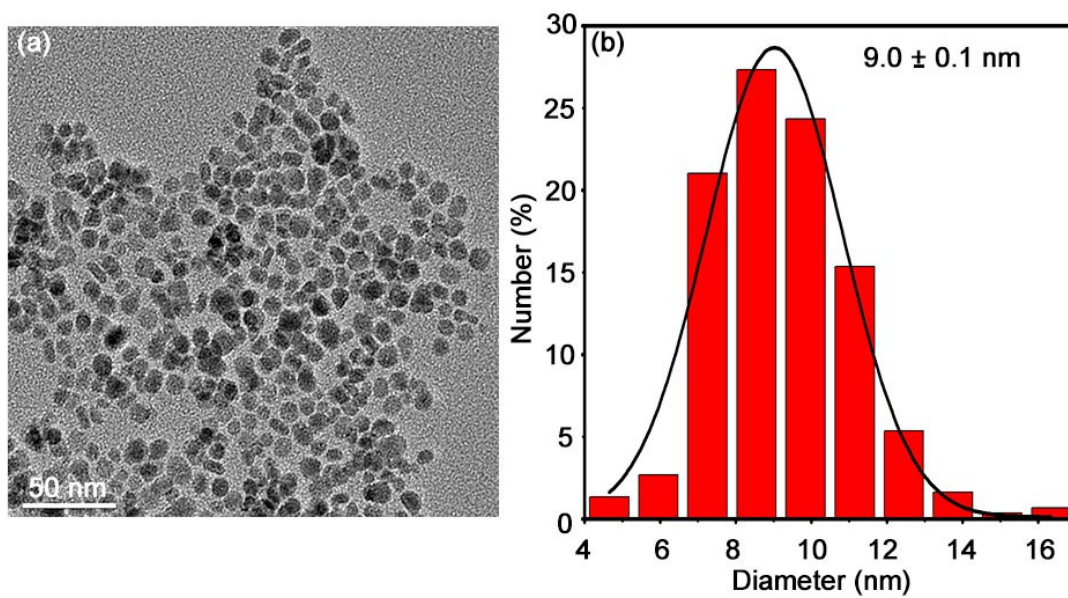


**Fig. S10** TEM images of Cu-Ag<sub>2</sub>S/PVP NPs (a) and the corresponding size distribution histograms (b).



### SI-1 Calculation for molar extinction coefficient:

The molar extinction coefficient ( $\epsilon$ ) of Cu-Ag<sub>2</sub>S/PVP NPs at 808 nm could be calculated by the following equations:

$$\epsilon = \left( A \frac{\pi}{6} d^3 \rho N_A \right) / (LC_{wt})$$

where  $A$ ,  $d$ ,  $\rho$ ,  $N_A$ ,  $L$  and  $C_{wt}$  are the absorbance at 808 nm, the average diameter of nanospheres, the density of nanospheres, Avogadro's constant, the pathlength through the sample and the weight concentration of the nanospheres, respectively. The absorbance value is 1.055 at 808 nm when Cu-Ag<sub>2</sub>S/PVP NPs with Cu concentration of 100 ppm (Figure S7). The average diameter of nanospheres is 9.0 nm (Figure S8). The density  $\rho$  for bulk Ag<sub>2</sub>S is about 7.23 g cm<sup>-3</sup>. The density of Cu-Ag<sub>2</sub>S/PVP NPs was approximately replaced by the bulk one.  $L$  is equal to 1 cm. Therefore the molar extinction coefficient is about  $1.8 \times 10^7 \text{ M}^{-1} \text{ cm}^{-1}$ . In comparison with Cu-Ag<sub>2</sub>S/PVP NPs, the molar extinction coefficient of Cu<sub>2-x</sub>S/PVP NPs in this work is only about  $2.6 \times 10^6 \text{ M}^{-1} \text{ cm}^{-1}$ .

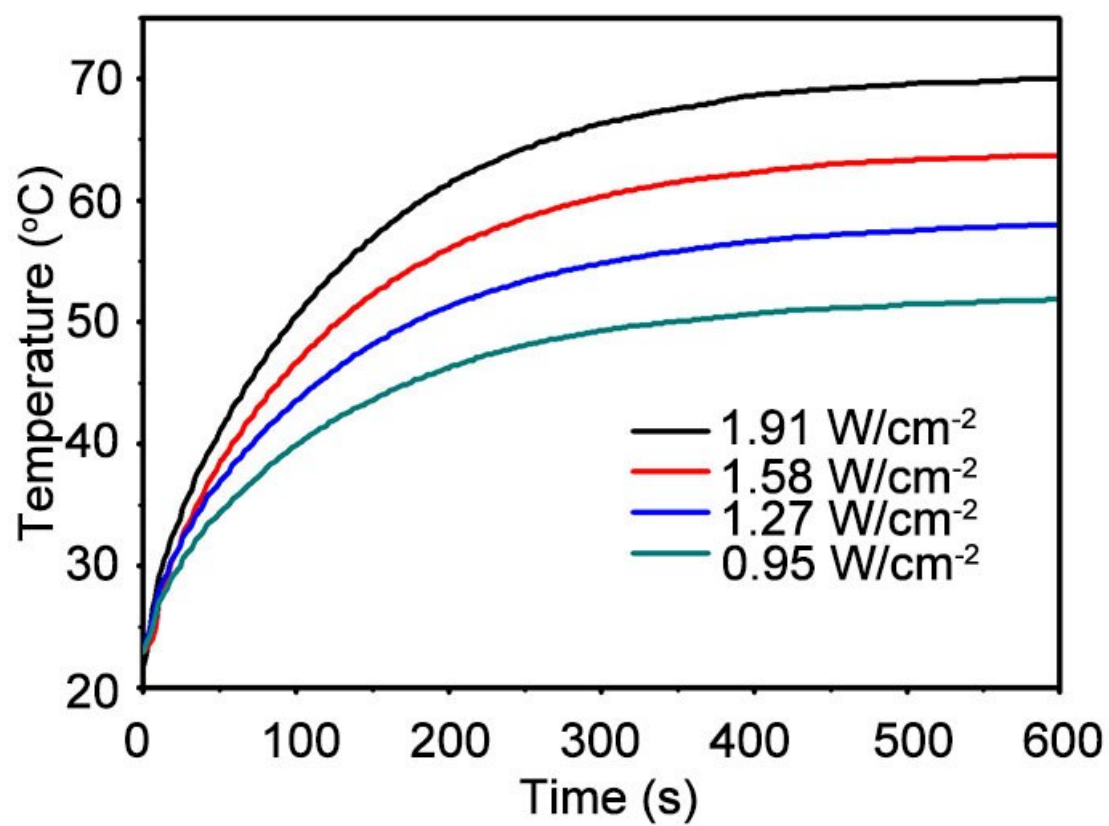


**Fig. S11** Temperature elevation profiles of PBS solution containing Cu-Ag<sub>2</sub>S/PVP NPs (Cu concentration: 100 ppm) upon 808 nm laser irradiation with different power density.

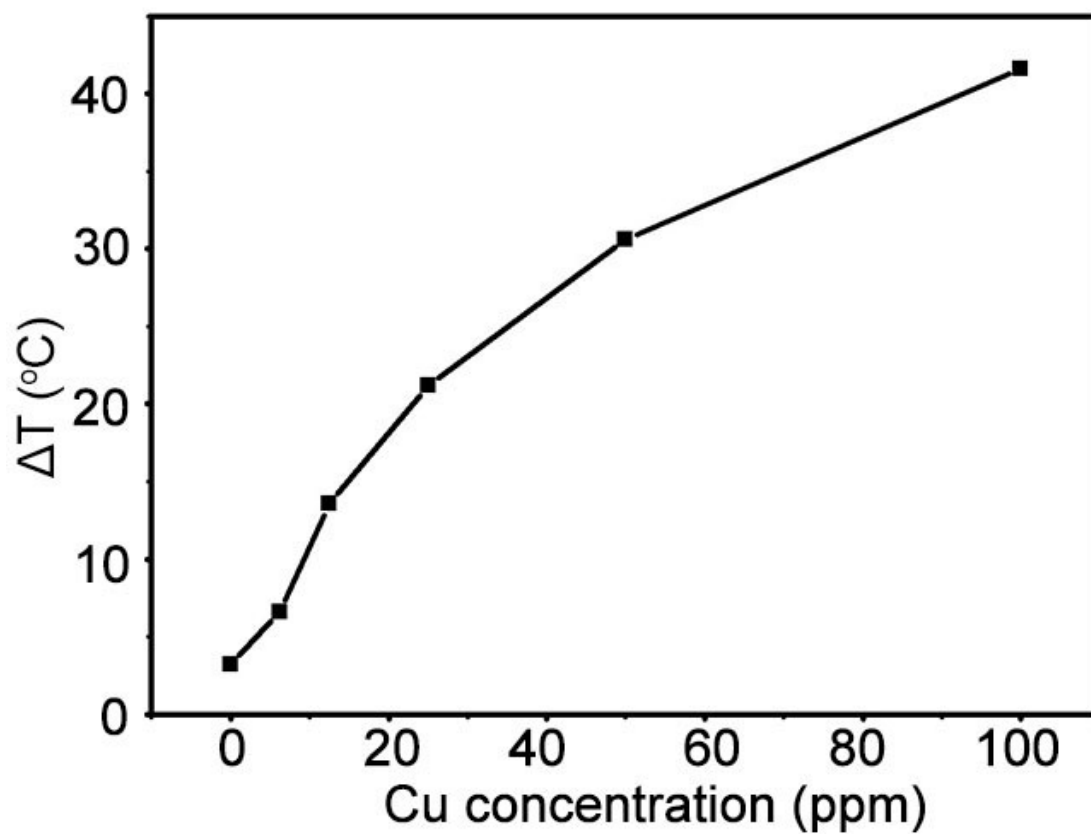


**Fig. S12** The temperature increase ( $\Delta T$ ) of PBS solution containing Cu-Ag<sub>2</sub>S/PVP NPs with various Cu concentrations upon 808 nm laser irradiation (1.58 W cm<sup>-2</sup>, 10 min).

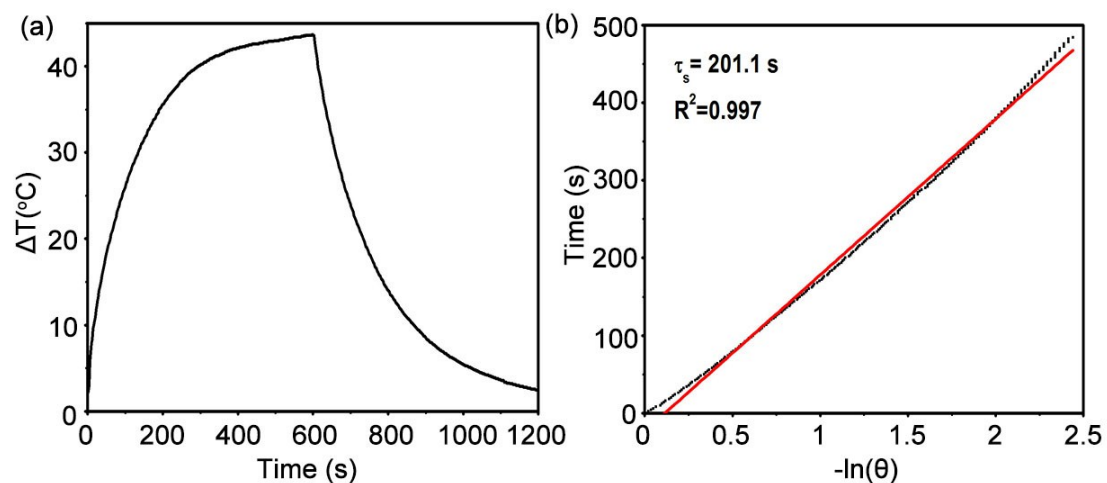


**Fig. S13** (a) Temperature elevation profiles of PBS solution containing Cu-Ag<sub>2</sub>S/PVP NPs (Cu concentration: 100 ppm) upon 808 nm laser irradiation (1.58 W cm<sup>-2</sup>, 10 min) and then the laser was shut off. (b) Plot of the cooling time versus  $-\ln(\theta)$  obtained from the cooling stage as shown in (a).

## SI-2 Calculation for photothermal conversion efficiency:

The photothermal conversion efficiency ( $\eta$ ) could be calculated by the following equations:

$$\eta = \frac{hS(T_{\max} - T_{\text{surr}}) - Q_{\text{dis}}}{I(1 - 10^{-A_{808\text{nm}}})} \quad (1)$$

where  $h$ ,  $S$ ,  $T_{\max}$ ,  $T_{\text{surr}}$ ,  $Q_{\text{dis}}$ ,  $I$ , and  $A$  are heat transfer coefficient, irradiated area, the equilibrium temperature, the ambient temperature of the surroundings, the heat dissipation from the light absorbed by the quartz sample cell, the laser power density, and absorption of Cu-Ag<sub>2</sub>S/PVP NPs at 808 nm, respectively. The value of  $hS$  is calculated by using the following equation (2) to (4):

$$hS = \frac{\sum m_i C_{p,i}}{\tau_s} \quad (2)$$

$$t = -\tau_s \ln \theta \quad (3)$$

$$\theta = \frac{T - T_{\text{surr}}}{T_{\max} - T_{\text{surr}}} \quad (4)$$

where  $m$ ,  $C_p$ ,  $t$ ,  $\tau_s$  are the mass of sample, the thermal capacity of sample, cooling time after irradiation, and the sample system time constant, respectively. The  $Q_{\text{dis}}$  was measured independently using a quartz cuvette cell containing PBS without Cu-Ag<sub>2</sub>S/PVP NPs. The value of  $Q_{\text{dis}}$  is calculated by using the following equation:

$$Q_{\text{dis}} = hS(T_{\max, \text{PBS}} - T_{\text{surr, PBS}})$$

The  $T_{\max}$ ,  $T_{\text{surr}}$ , and  $\tau_s$  was obtained from Figure S11 to be 64.8 °C, 21.2 °C, and 201.1s, The value of  $m$  and  $C_p$  are 1g and 4.2 J/(g•°C). Therefore,  $hS$  is calculated to be 20.89 mW/°C. The value of  $T_{\max}-T_{\text{surr}}$  equals 43.6 °C,  $Q_{\text{dis}}$  and  $A_{808\text{nm}}$  are measured independently as 66.83 mW with power density ( $I$ ) 1.58 W/cm<sup>2</sup> and 1.055, respectively. Substituting all of value to parameters into the equation (1), photothermal conversion efficiency ( $\eta$ ) of Cu-Ag<sub>2</sub>S/PVP NPs can be calculated to be 58.2%. In comparison with Cu-Ag<sub>2</sub>S/PVP NPs, the photothermal conversion efficiency of Cu<sub>2-x</sub>S/PVP NPs is about 27.1%.

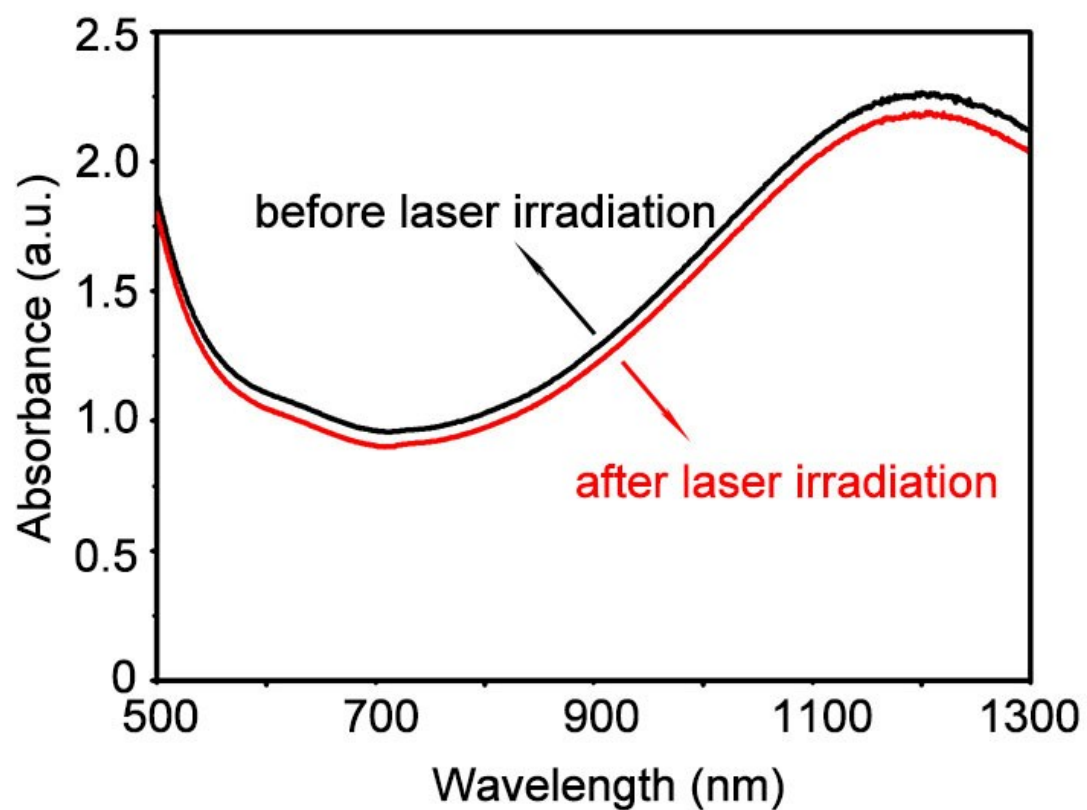


**Fig. S14** The UV-vis-NIR absorption spectrum of PBS solution containing Cu-Ag<sub>2</sub>S/PVP NPs (Cu concentration: 100 ppm) before and after 808 nm laser irradiation (1.58 W cm<sup>-2</sup>, 60 min).

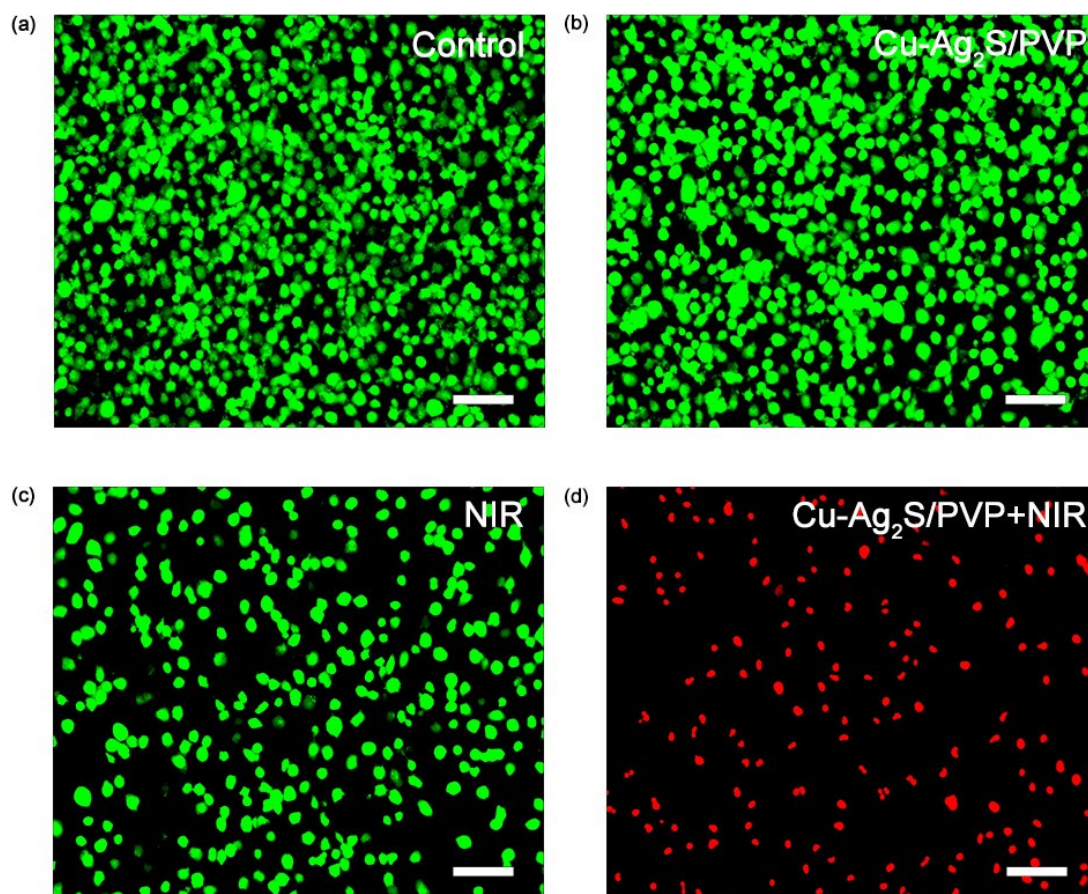


**Fig. S15** Live–dead staining images of 4T1 murine breast tumor cells incubated with or without PBS solution containing Cu-Ag<sub>2</sub>S/PVP NPs (Cu concentration: 200 ppm) upon 808 nm laser irradiation ( $1.58 \text{ W cm}^{-2}$ , 10 min). All the scale bars are 200  $\mu\text{m}$ .



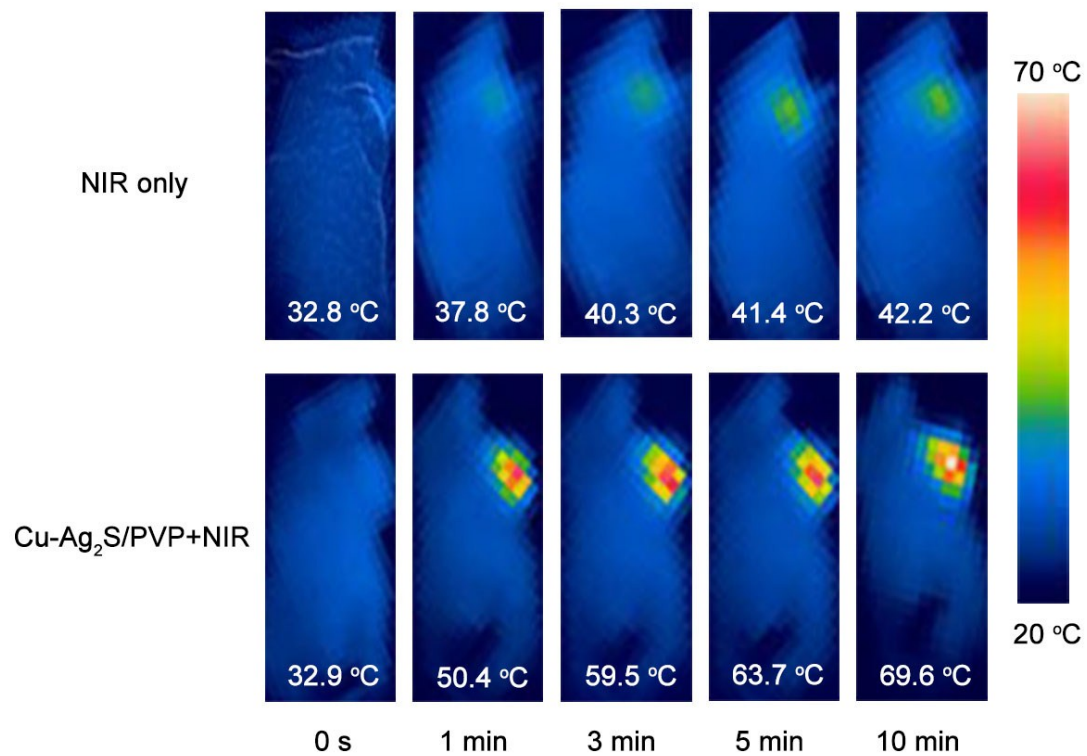


**Fig. S16** Photothermal images of tumor-bearing mice recorded during the laser irradiation after intratumoral injection of PBS or PBS solution containing Cu-Ag<sub>2</sub>S/PVP NPs (100  $\mu$ L, 200 ppm).

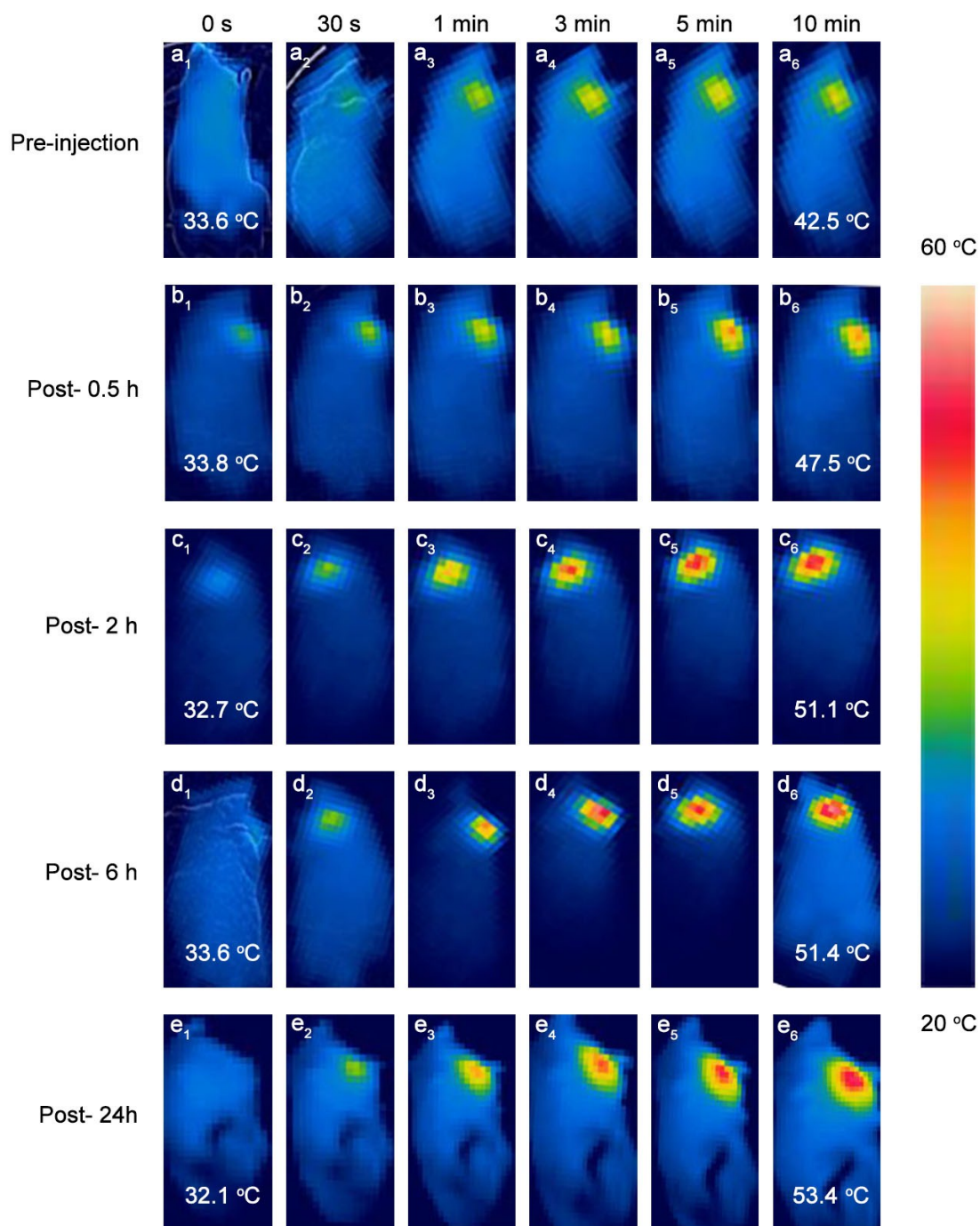


**Fig. S17** Photothermal images of tumor-bearing mice recorded during the laser irradiation after intravenous injection of PBS solution containing Cu-Ag<sub>2</sub>S/PVP NPs (100  $\mu$ L, 200 ppm) taken at different time intervals.

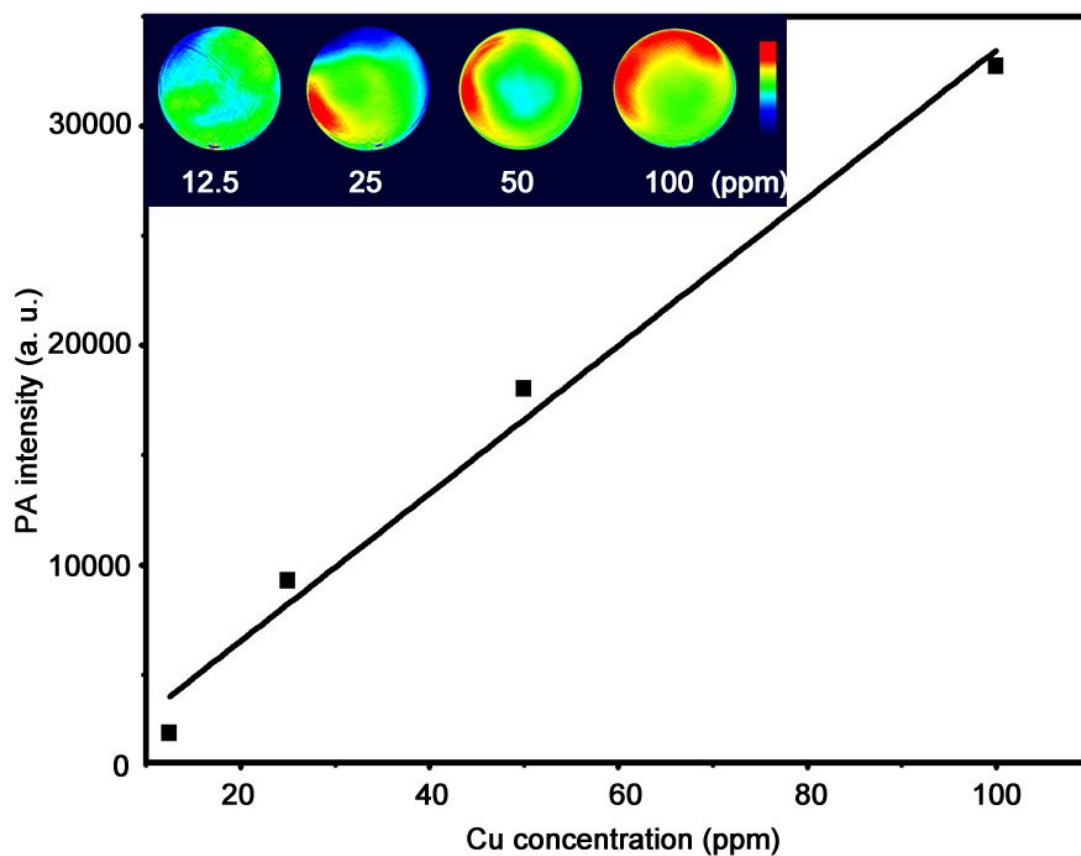


**Fig. S18** Linear fitting plots of PA amplitudes versus Cu concentrations of Cu-Ag<sub>2</sub>S/PVP NPs PBS solution under 808 nm laser irradiation. The inset is the PA image of agar gel cylinder at versus Cu concentrations of Cu-Ag<sub>2</sub>S/PVP NPs PBS solution.

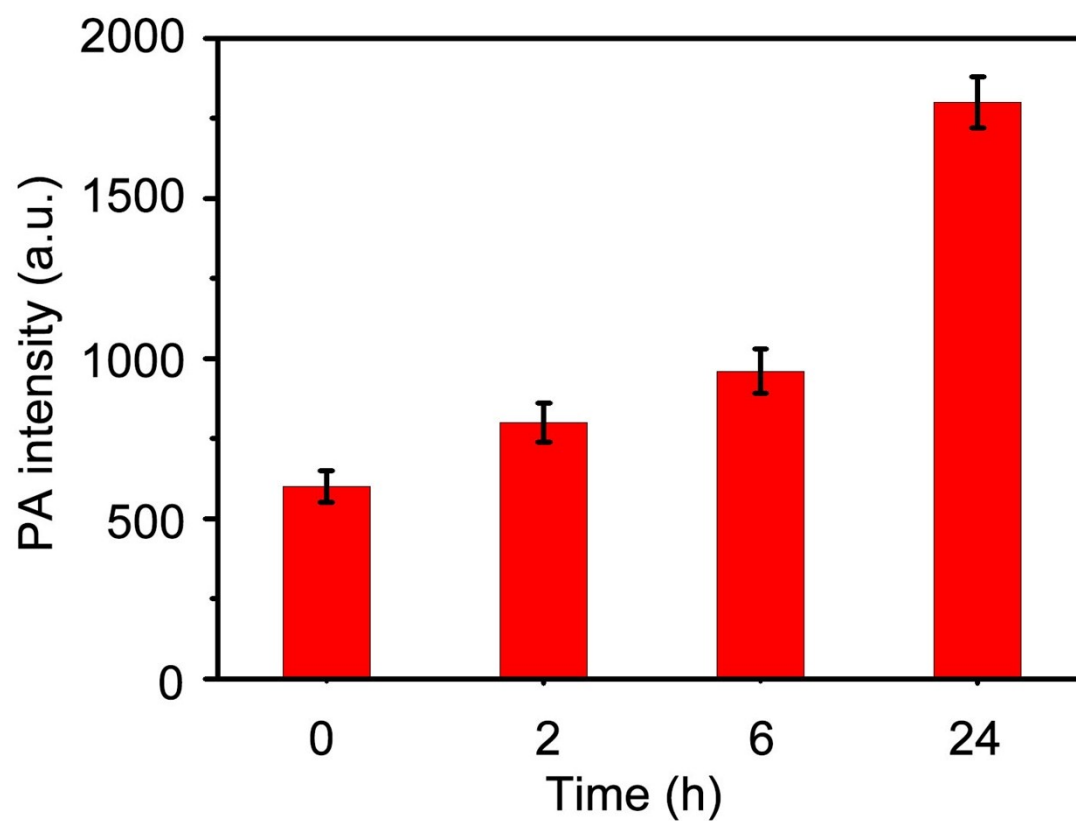


**Fig. S19** The quantitative PA intensity of the tumor corresponding to the given time points (0, 2, 6, and 24 h).

**Table S1.** The content of Cu and Ag in feces or urine at different time points (2 h, 6 h, 1d, 3 d, and 7 d) after intravenous injection of PBS solution containing Cu-Ag<sub>2</sub>S/PVP NPs.

Post-injection	0 h	2 h	6 h	1 d	3 d	7 d
Content of Cu in Feces (µg/g)	5.2	9.93	13.13	20.76	17.84	9.91
Content of Cu in Urine (µg/mL)	0.53	0.63	0.92	2.26	1.36	0.44
Content of Ag in Feces (µg/g)	0.08	0.08	0.09	0.53	0.35	0.11
Content of Ag in Urine (µg/mL)	0.01	0.02	0.02	0.09	0.04	0.02

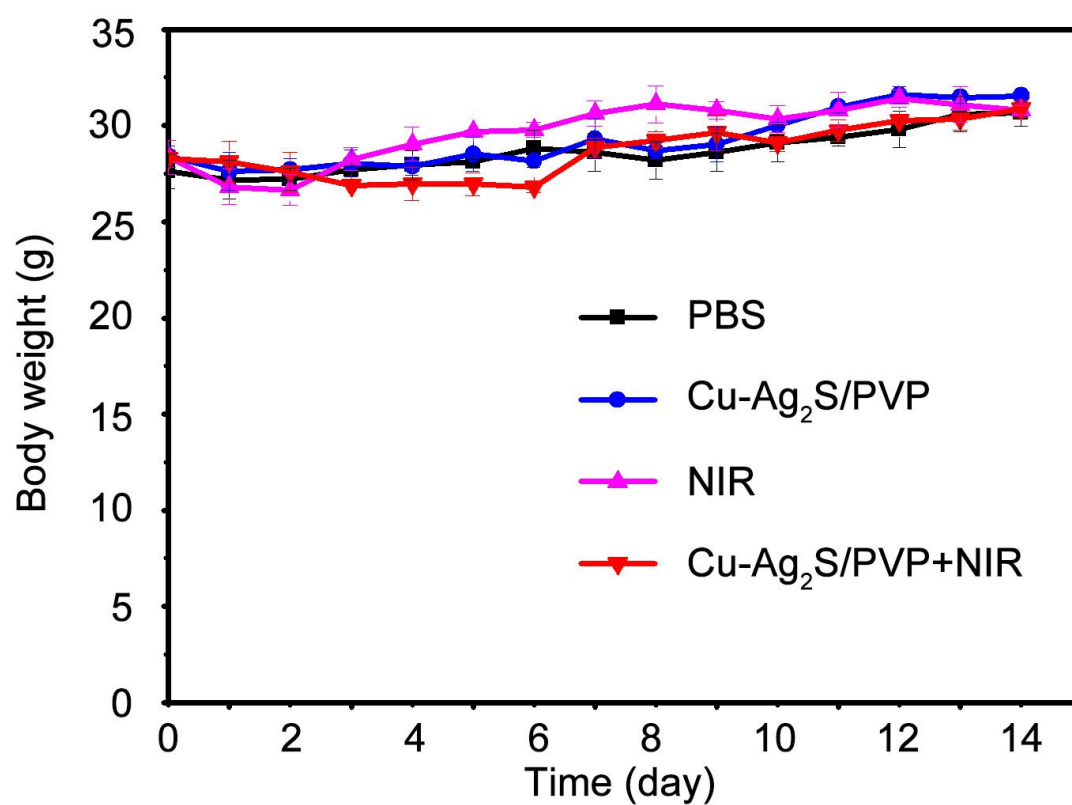


**Fig. S20** Body weight of tumor-bearing mice after treatment with PBS, Cu-Ag<sub>2</sub>S/PVP, NIR, and Cu-Ag<sub>2</sub>S/PVP+NIR, respectively.

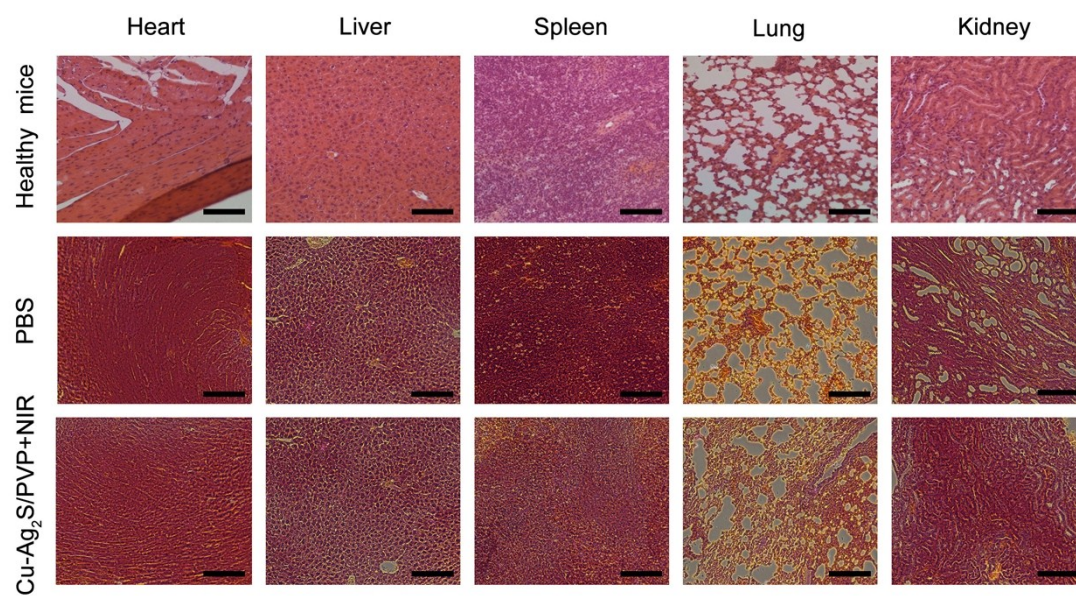


**Fig. 21** Histological analysis of the heart, liver, spleen, lung, and kidney obtained from group I, group IV, and healthy mice. All the scale bars are 100  $\mu$ m.

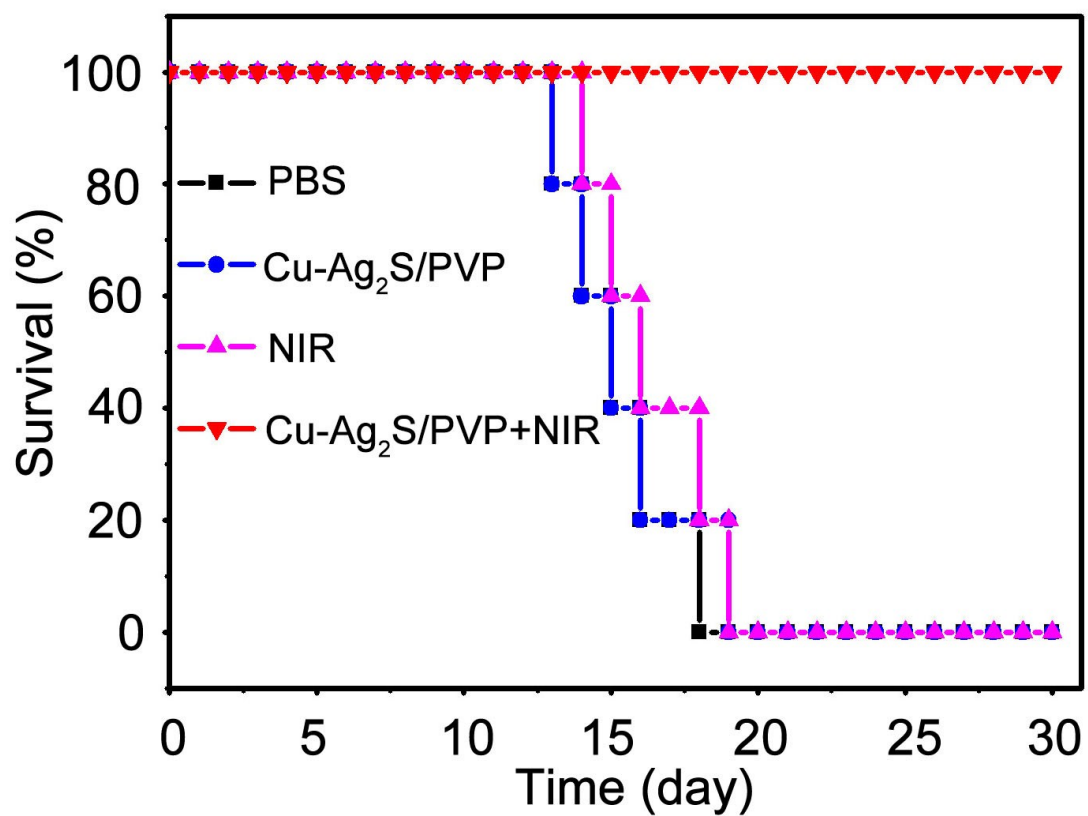


**Fig. 22** Survival rates of four groups of tumor-bearing mice ( $n = 5$ ) as a function of time post-treatments.